BBA - Bioenergetics 1860 (2019) 317–324

Contents lists available at ScienceDirect

BBA - Bioenergetics

journal homepage: www.elsevier.com/locate/bbabio

Chemical rescue of H^+ delivery in proton transfer mutants of reaction center of photosynthetic bacteria

Péter Maróti*

Institute of Medical Physics, University of Szeged, Hungary

ARTICLE INFO

Keywords:
Bacterial photosynthesis
Reaction center protein
Light-induced proton delivery
Proton transfer mutants
Chemical rescue

ABSTRACT

In the native and most mutant reaction centers of bacterial photosynthesis, the electron transfer is coupled to proton transfer and is rate limiting for the second reduction of $Q_B^- \rightarrow Q_BH_2$. In the presence of divalent metal ions (e.g. Cd^{2+}) or in some ("proton transfer") mutants (L210DN/M17DN or L213DN), the proton delivery to Q_B^- is made rate limiting and the properties of the proton pathway can be directly examined. We found that small weak acids and buffers in large concentrations (up to 1 M) were able to rescue the severely impaired proton transfer capability differently depending on the location of the defects: lesions at the protein surface (proton gate H126H/H128H + Cd^{2+}), beneath the surface (M17DN + Cd^{2+}, L210DN/M17DN) or deep inside the protein (L213DN) could be completely, partially or to very small extent recovered, respectively. Small zwitterionic acids (azide/hydrazoic acid) and buffers (tricine) proved to be highly effective rescuers consistent with their enhanced binding affinity and access to any of the proton acceptors (including Q_B^- itself) in the pathway. As a consequence, back titration of the protons at L212Glu could be observed as a pH-dependence of the rate constant of the charge recombination in the presence of azide or formate. Model calculations support the collective influence of the acid cluster on the change of the protonation states upon extension of the cluster with the bound small acid. In proton transfer mutants, the rescuing agents decreased the free energy of activation together with their enthalpic and entropic components. This is in agreement with the hypothesis that they function as protein-penetrating protonophores delivering protons into the chain and select dominating paths out of many alternate routes. We estimate that the proton delivery will be accelerated in one pathway out of 100–200 alternate pathways. The implications for design of the chemical recovery of impaired intra-protein proton transfer pathways in proton transfer mutants are discussed.

1. Introduction

The transfer of H^+ ions in energy transducing proteins (carbonic anhydrase [1], bacteriorhodopsin and channelrhodopsin [2], cytochrome *c* oxidase [3,4] or photosynthetic reaction center (RC) [5]) is a fundamental process in diverse fields of bioenergetics of respiration or photosynthesis [6]. A network of ionizable amino acids and bound water molecules extended from the exterior to the catalytic site promote long range (~20 Å), fast and efficient intra-protein proton transfer [7–9]. Based on X-ray data, mutational studies and electrostatic calculations, the pathway has been resolved with high precision in the bacterial photosynthetic RC [10,11].

In RC of *Rhodobacter sphaeroides* the proton transfer is coupled to electron transfer to the secondary ubiquinone, Q_B, whose reduction cycle is driven by two sequential light-activated turnovers of the RC. The first light reaction ($\Rightarrow$) results in charge separation between the BChl dimer P and the primary quinone Q_A followed by concomitant proton uptake of the nearby carboxylic group L212Glu and electron transfer to Q_B:

$$P(Q_AQ_B)Glu^- \Rightarrow P^+(Q_A^-Q_B)Glu^- \overset{H^+,e^-}{\leftrightarrow} P^+(Q_AQ_B^-)GluH \quad (1)$$

The significant and exclusive light-induced IR signal of L212Glu points to a specific tuning for allocating the proton uptake specifically to this carboxylic acid [11].

The new charge separation after the second light-induced turnover is followed also by a two step process in which fast protonation of Q_B^- via L223Ser [12–14] precedes the rate limiting electron transfer to Q_B^-H:

Abbreviations: ET, electron transfer; P, bacteriochlorophyll dimer; Q_A and Q_B, primary and secondary quinone acceptors, respectively; RC, (bacterial) reaction center

* Rerrich Béla tér 1, Szeged H-6720, Hungary.
E-mail address: pmaroti@sol.cc.u-szeged.hu.

https://doi.org/10.1016/j.bbabio.2019.01.006
Received 24 May 2018; Received in revised form 5 December 2018; Accepted 25 January 2019
Available online 29 January 2019
0005-2728/

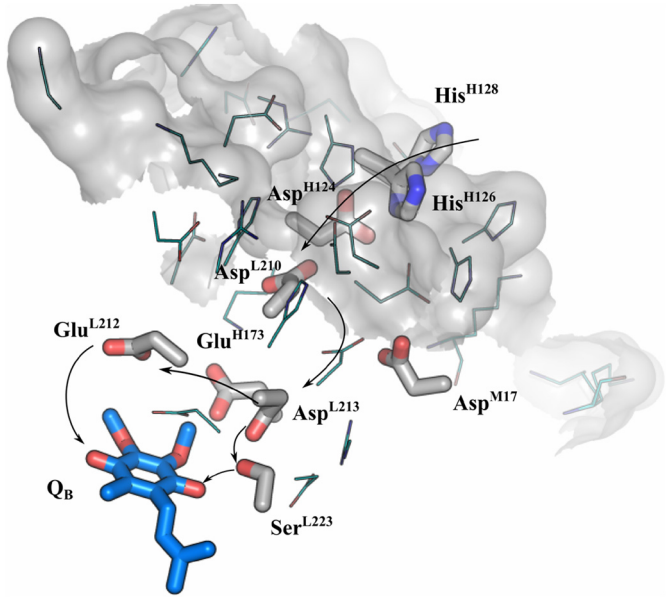

Fig. 1. Dominant proton delivery pathway from the aqueous bulk phase to Q_B in RC from *Rba. sphaeroides*. The protons enter the proton gate constituting of surface residues AspH124, HisH126 and HisH128, pass via Asp-L210 and/or Asp-M17 to proceed to Asp-L213 where they diverge and get to the carbonyl oxygen atoms of Q_B via SerL223 (first H^+) or GluL212 (second H^+). The grey contoured surface encloses surface of the RC. All residues of the acidic cluster are buried. The figure was prepared in VMD; structure file was 1dv3.pdb.

$$Q_AQ_B^- \Rightarrow Q_A^-Q_B^- \overset{H^+}{\leftrightarrow} Q_A^-Q_BH \overset{e^-}{\rightarrow} Q_AQ_BH^- \quad (2)$$

L223Ser does not form direct interactions with the neutral quinone and its role as proton donor to Q_B is mediated by the formation of the semiquinone or biradical [15]. Subsequent internal proton transfer from the protonated L212Glu leads to the formation and release of the quinol Q_BH_2.

The proton transfer extends from the aqueous bulk surface to the deeply buried Q_B over a distance of 13–15 Å (Fig. 1). The region involves a large cluster of acidic and polar residues, which can be the constituents of several possible proton delivery pathways. While residues close to Q_B (L212Glu, L213Asp and L223Ser) are true proton carriers as terminal members of the pathway, others, most likely do not play an active proton-carrying role but set the local electrostatics and p*K* values of the members of the cluster. In wild type RCs, the proton transfer occurs through the dominant pathway from the proton entry point (H126His/H128His) to Q_B via L213Asp with rate much larger than that of any coupled electron transfer steps in Eqs. (1) and (2). However, when key residues in the proton transfer pathways are mutated, alternate pathways will save the proton transfer in expense of severe (orders of magnitude) reduction of the rate. These "proton transfer mutants" are highly valuable species to determine the rate of proton transfer which becomes the rate limiting step of the measured electron transfer reactions in these species [16] and they permit the study of the role and significance of the alternate proton pathways [17].

Some second site (revertant) mutations remote from Q_B can restore the proton transfer rate close to that of the wild type. They cause yet unspecified structural changes that propagate a "domino-effect" over relatively long distances to L213Asp or to Q_B and activate alternate proton pathways [17–19]. In another approach, the substantially impaired rate of proton transfer was chemically restored upon adding high concentrations of imidazole (double mutant H126HA/H128HA, [20]) or of small, neutral weak acids (double mutant L210DN/M17DN, [21]). The Brönsted plots of activity versus pK_a of the rescuing acids were linear with a slope of −1 both in H126HA/H128HA [20] and L210DN/M17DN [21] double mutants. The pK_a value of the extrapolated diffusion limited rate constant corresponded to that of a carboxylic acid in the cluster or of Q_B^- itself [22,23].

The combination of site-directed mutagenesis and chemical rescue of proton transfer has proved to be successful not only in the RC of photosynthetic bacteria, but in other proteins as well. The experimental strategy is widely used to understand the chemical and structural requirements for efficient catalysis in carbonic anhydrase enzymes [24], cytochrome *c* oxidase [25], heme-containing proteins [26] and photosynthetic RC of photosystem II of higher plants [27]. The power of the method is indicated by the possibility to modulate the activity of specific enzymes in vivo, and even to reactivate genetically defective enzymes that might have prospective futures in therapy [28].

The objective of this study is to experimentally probe the structural basis for the functional differences in the rates of H^+ translocation between heavily impaired and chemically rescued RCs with a special emphasis on the role of the alternate pathways. This is accomplished by specific mutations at several crucial points of the dominant pathway to block there the proton delivery. The molecular constraints will be set up either at the entrance (blocking the H124-H126 "proton gate" by divalent metal ions [29,30]) or below the protein surface (L210DN/M17DN mutations [21]) or deep inside the RC (L213DN mutation [31]). These modifications severely (by orders of magnitude) reduce the rate of proton delivery and thus become the rate limiting step of the measured rate of the second electron transfer $k(2)$. Small acids, buffers and salts of large concentrations are able to increase $k(2)$ approximately to a value observed in wild type RC [20,21]. By discussion of the structural and energetic mechanisms of the chemical rescue, we try to reveal the molecular background of the rescue and whether this rescue occurs through recovery of the proton-carrying function of the mutated site in the dominant pathway and/or through activation of alternate pathways.

2. Materials and methods

2.1. Reaction centers, reagents and kinetics

Details of the molecular biological techniques in generating *Rhodobacter* (*Rba.*) *sphaeroides* with mutant RCs have been described earlier [21,31]. RCs were isolated by detergent fractionation of the chromatophore with 0.7% lauryl (dodecyl) dimethylamine-N-oxide (LDAO) (Fluka), followed by ammonium sulfate precipitation, and column purification using DEAE-Sephacel (Sigma) [32]. The RC was concentrated to ~100 μM by centrifugation (Amicon Centricon-30). To exchange the detergent, the RC was dialyzed 1–2 days at 4 °C against 1 mM Tris buffer (pH 8.0) and 0.03% Triton X-l00 detergent. Isolated RCs typically displayed A280/A800 optical ratio (purity) of 1.3.

Ubiquinone-10 solubilized in ethanol was added in large excess ([UQ]/[RC] > 10) to RC to reconstitute the secondary quinone activity checked by the ratio of the amplitudes of the slow and fast components of the charge recombination. Ethanolic solutions of exogenous donors (ferrocene, ethyl ferrocene and DAD (diaminodurene)) to reduce P^+ were prepared fresh prior use. Cytochrome-*c* (horse heart grade VI) was reduced (> 95%) by hydrogen gas on platinum black and filtered (0.2 μm pore size acetate filter). A cocktail (2–2 mM each) of buffers (citric acid, Mes, Mops, Pipes, Tris, Ches and Caps) were used to stabilize the pH value of the solution.

The kinetics of the charge recombination after the first flash, $P^+(Q_AQ_B)^- \rightarrow P(Q_AQ_B)$ was measured at 430 nm and were fit to the sum of two exponentials representing the fast ($P^+Q_A^- \rightarrow PQ_A$) and slow ($P^+Q_AQ_B^- \rightarrow PQ_AQ_B$) components. The kinetics of the second electron transfer, $Q_A^-\ Q_B^- \rightarrow Q_AQ_BH^-$ were measured at 450 nm, following the second of two short flashes 0.5 s apart, in the presence of exogenous electron donor to P^+. The kinetics were analyzed by a two-component exponential fit, representing the second electron transfer and the re-reduction of P^+ by the exogenous donor seen at the same wavelength [22,23]. The electron donor had to re-reduce P^+ before the second

flash, and its kinetics had to be also separated from that of the second electron transfer. Because the observed electron transfer rate varied widely with experimental conditions (pH, temperature), the donors and their concentrations had to be adjusted to separate the two effects. Cytochrome-c^{2+} is a fast donor (halftime < 100 μs), but could have slower component (~1 ms) that might coincide with the electron transfer. Ferrocene at large (150–200 μM) concentration showed a halftime of ~2 ms and ethyl ferrocene at low (2–4 μM) concentration could reduce P^+ with halftime of 200–500 ms. The second electron transfer kinetics were well fit by a single component. When the temperature was not defined, the kinetic measurements were carried out at 21 °C.

2.2. Analysis of the activation parameters

The temperature (T)-dependence of the rates of the second electron transfer $k^{(2)}$ were measured in different mutants under various treatments and plotted as $\ln(k^{(2)}h/(k_BT))$ versus $1/T$ (Eyring plot). In proton transfer mutants of the RC, the observed $k^{(2)}$ is controlled not by the rate of interquinone electron transfer but that of the proton transfer to Q_B^-. The thermodynamically related Eyring rate equation for the activated complex state can be written as.

$$k^{(2)} = \kappa \cdot \frac{k_B T}{h} \exp\left(-\frac{\Delta G_0^{\#}}{RT}\right) \quad (3)$$

where κ is the transmission coefficient (assumed to be 1), k_B, h and R are the Boltzmann's, Planck's and universal gas constants, respectively, and $\Delta G_o^{\#} = \Delta H_o^{\#} - T\cdot\Delta S_o^{\#}$, where $\Delta G_o^{\#}$, $\Delta H_o^{\#}$ and $\Delta S_o^{\#}$ are the changes of free energy, enthalpy and entropy of activation, respectively. These energies relate to the transition to the activated state of the rate-limiting proton transfer step. As such, $\Delta H_o^{\#}$ is closely related to the height of the energy barrier of the activated-state complex, and the entropy of activation ($\Delta S_o^{\#}$) relates to the ratio between the numbers of available configurations of the activated complex to those of the reactants. The various energies of activation (free, enthalpy, and entropy) for the activated complex were calculated from the measured temperature-dependence of the rates by least square linear fit using Eq. (3). The slope and intersection of the straight line were directly related to the changes of the enthalpy of activation and of the entropy of activation, respectively.

2.3. Calculation of the probability of protonation in the acidic cluster

The dominating proton delivery pathway to Q_B consists of n closely connected acidic residues which are neutral when protonated (with binary number 0) and anionic when deprotonated (with binary number 1). According to Cheap et al. [17], the probability of a particular protonation configuration of the cluster (k) can be calculated by.

$$P_k(\mathrm{pH}) = \frac{10^{\boldsymbol{B}_k\cdot(\boldsymbol{M}(\mathrm{pH})\cdot\boldsymbol{B}_k)}}{\sum_{i=0}^{2^n-1} 10^{\boldsymbol{B}_i\cdot(\boldsymbol{M}(\mathrm{pH})\cdot\boldsymbol{B}_i)}}, \quad (4)$$

where $\boldsymbol{B}_i$ is the vector whose elements are the binary digits of number i, $\boldsymbol{M}$(pH) is the $n \times n$ matrix whose nondiagonal elements are $E_{ij}/2$ and diagonal elements are (pH − pK_i). Here E_{ij} denotes the mutual interaction energy between charged groups i and j expressed in units of RT ln (10) ≈ 60 meV (at room temperature). They increase the corresponding intrinsic pK_a values of the residues. The (right and left) scalar products with vector $\boldsymbol{B}$ (indicated by dots) select the interaction terms corresponding to all couples of charged groups. From the calculated probabilities of all k configurations, it is straightforward to determine the probability of protonation of a selected residue in the cluster. MathCad 14.0 was used for the numerical calculations.

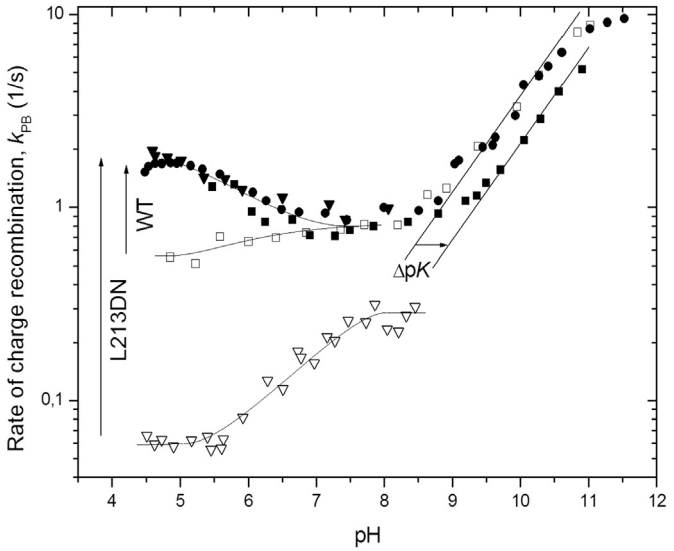

Fig. 2. Effect of small acids (azide and formate) on pH-dependence of the rate constant of $P^+Q_B^- \rightarrow PQ_B$ charge recombination in RC of wild type (WT) and L213DN mutant with indicated extent and region of back titration (arrows) and pK shift (ΔpK) induced by azide. Symbols: □ (WT, 500 mM NaCl), ■ (WT, 500 mM azide), • (WT, 500 mM formate), ∇ (L213DN) and ▼ (L213DN, 500 mM azide). Conditions: 1.8 μM RC, 40 μM UQ_{10}, 0.02% TX and 2–2 mM mixture of buffers (succinic acid, Mes, Mops, Tris and Caps).

3. Results

3.1. Charge recombination: deviation from the general salt effect

Various salts, including some weak acids in large concentration stimulated the second electron transfer [20,21]. The effect was not of purely ionic origin and the increase of penetration of the protein by H^+ ions was not due to charge screening. The influence of azide and formate ions on pH-dependence of the rate of charge recombination can be also distinguished from the general salt effect, whereas addition of NaCl of the same ionic strength (500 mM) had very little (if any) effect (Fig. 2). The rate constant of the back reaction k_{PB} in wild type (WT) RC is roughly pH independent between pH 6.5 and 8, but steeply increases at higher pH and slightly decreases at lower pH. It is a sensitive indicator of the protonation state of L212Glu and the electrostatics created by the cluster of ionizable residues in the vicinity of Q_B [33]. FTIR studies clearly indicated that L212Glu undergoes changes in partial ionization at pH 8.0 and is primarily responsible for the pH dependence at pH > 8.0 (see Eq. (1) and [11]). The pH dependence of k_{PB} at pH < 6 reflects the ionization behavior of strongly coupled response of AspL213 and AspL210 in the cluster [31]. A significant increase of k_{PB} upon addition of both azide and formate can be observed below pH = 6.5. These small acids induce change in the protonation property of the cluster which is manifested as experimental evidence of back titration of L212Glu: by decrease of pH, the protonation state of L212Glu does not increase but decreases in the acidic pH range. Additionally, azide causes a pK shift of +0.5 pH units in the high pH region, and therefore can directly influence the electrostatics of the cluster. However, the formate does not induce a pK shift, thus it has no electrostatic influence on these residues. The changes of the pH-dependence of k_{PB} upon addition of small acids exemplify the complex interactions in the Q_B region of the protein.

A similar tendency of back titration as observed in wild type RCs can also be observed in the L213DN mutant RC. The charge recombination becomes significantly slower than that of WT. The smaller k_{PB} value (larger stabilization of the electron at Q_B than at Q_A) can be attributed to the increased protonation state of L212Glu in the mutant. The L212Glu and L213Asp may be best considered as one group that is

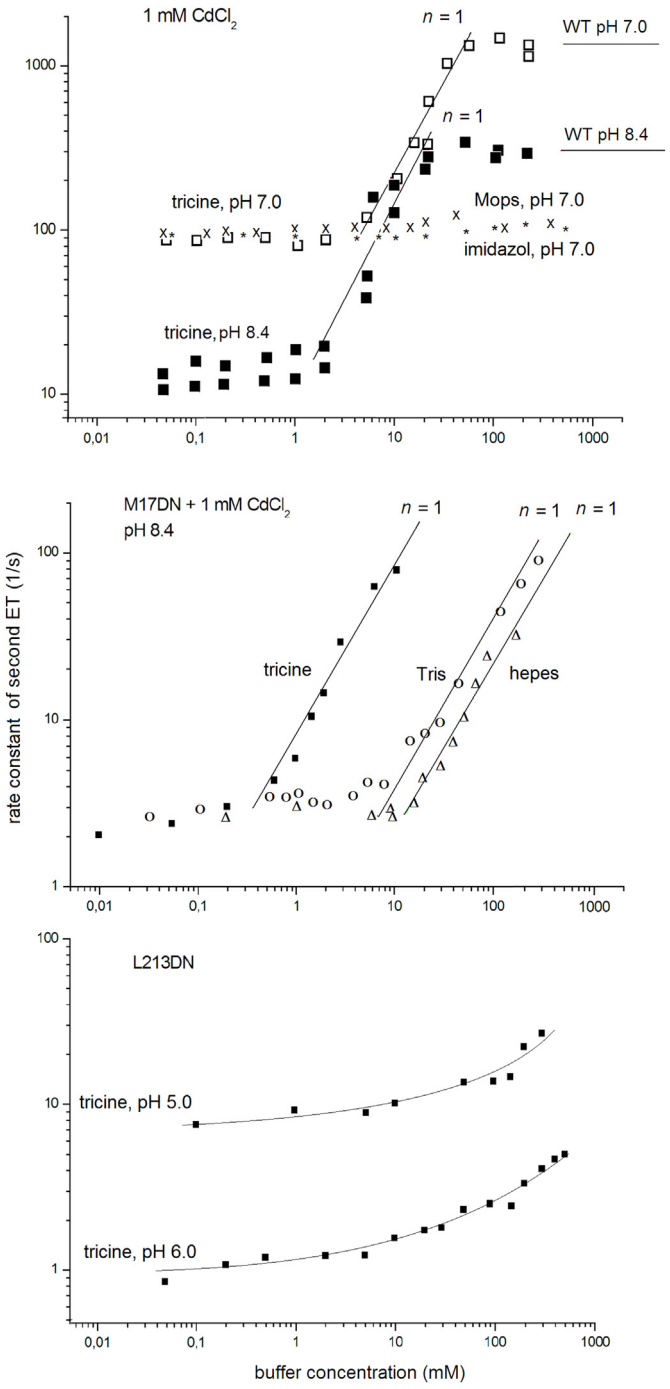

Fig. 3. Rescue of proton transfer by buffers in RC of disabled transfer pathway at the surface proton gate only (1 mM $CdCl_2$, top panel), at combined places of the surface and beneath the surface of the protein (1 mM $CdCl_2$ and M17DN, middle panel) and deep inside the protein (L213DN, bottom panel). In these cases, the proton transfer became the bottle neck of the measured second electron transfer (ET). The WT values of rate constants are indicated by horizontal lines (top). Symbols: □ (tricine, pH 7.0), x (Mops, pH 7.0), * (imidazol, pH 7.0), ■ (tricine, pH 5.0, 6.0 and 8.4), o (Tris, pH 8.4) and Δ (hepes, pH 8.4). Conditions: 1.2 μM RC, 40 μM UQ_{10}, 0.02% TX, 20 mM KCl, 100–400 μM ferrocene (middle and bottom) and 20 μM cyt c^{2+} (top).

never more than singly ionized (less than singly protonated) at any pH [34]. In the absence of L213Asp, the H^+ ion is shifted entirely to L212Glu. Upon addition of azide, k_{PB} increases by more than one order of magnitude at pH 4.5 and the difference between the rate constants of the treated and untreated RC decrease progressively toward the higher pH values. We see that the small acid azide can reconstitute the pH-dependence of the charge recombination in L213DN mutant to the same level as observed in treated WT. The back titration demonstrates that azide preserves its general effect on the complex protonation configuration of the acidic cluster independently on the presence or absence of L213Asp.

3.2. Recovery of the second electron transfer

The impaired proton pathway to Q_B can be recovered by imidazole or other amine-containing acids in RC where the imidazole groups of the H126His and H128His of the proton gate were removed and replaced by Ala [20]. Depending on the location of the impairment and on the type of the buffer, other buffers are also able to restore the 2nd electron transfer partly or entirely (Fig. 3). If the proton entrance is blocked by a divalent cation Cd^{2+}, the rescue of the 2nd electron transfer can be initiated by ~1 mM concentration of tricine (pK_a = 8.05) at pH 8.4 and by somewhat larger (~5 mM) concentration at pH 7.0 (Fig. 3 top). Tricine restores the levels of the rate constants of the native RC completely following a straight line of slope n = 1 in double logarithmic representation. However, other buffers (Mops pK_a = 7.14 or imidazole pK_a = 6.95) are unable to rescue the 2nd electron transfer, although their pK_a values match the pH of the solution (pH = 7.0).

If the effect of Cd^{2+} at the surface of the RC is combined with the mutation of M17 beneath the surface (M17DN), the tricine shows nearly unchanged activity in restoration of the 2nd electron transfer at pH 8.4 (Fig. 3 middle). Other buffers as Tris (pK_a = 8.06) and hepes (pK_a = 7.48) are also able to rescue the proton transfer but at much (one order of magnitude, at least) larger concentration. They manage to alleviate the proton pathway damaged at and beneath the protein surface.

If the lesion occurs deep inside the protein (L213DN), then even tricine, the most effective buffer, will fail to rescue the proton delivery completely (Fig. 3 bottom). Although tricine can accomplish 4–5 times increase of the highly reduced rate constant of the mutant at the highest available concentration at pH 6, this is orders of magnitude smaller than that of the level of the native RC. At pH 5.0, the chemical rescue of the tricine is even weaker.

The separate defects at L210 and at M17 reduce the rate constant of the 2nd electron transfer but the single mutations are not proton transfer mutants. The combined (double) mutation L210DN/M17DN, however, makes the proton transfer rate-limiting in the 2nd electron transfer. Although the defects occur beneath the protein surface, the accessibility of the most effective small rescuing acids (azide and formate) is highly limited and the rescue is partial (Fig. 4). The initial slopes of n = 1 decrease gradually at increasing concentrations for both rescuing agents and the rescue has a tendency to saturate at values significantly smaller than that of the native RC. The azide is more effective than the formate both in concentration (about one order of magnitude) and probably in degree of rescue which is limited by the use of very high concentrations of the rescuing agents.

3.3. Changes of energies of activation caused by chemical rescue

The rescue agents accelerate the proton transfer to Q_B, and the kinetic changes involve energetic changes expressed in reduction of the free energy gap of the activated complex leading to $Q_A^-Q_BH^-$ (see Eq. (2)). The rate constants of the 2nd electron transfer are temperature dependent and the measured points fit to straight lines in Eyring representation with clear indications of the energetic effects of the chemical rescue (Fig. 5).

Conditions: 1.0 μM RC, 40 μM UQ_{10}, 0.02% TX, 5 mM NaCl, ferrocene (8 μM dimethyl ferrocene and 500 μM ethyl ferrocene, L213DN, pH 4.85) and 30 μM cyt c^{2+} (L210DN/M17DN, pH 7.50).

Upon addition of azide to L213DN mutant RC, not only the slope but

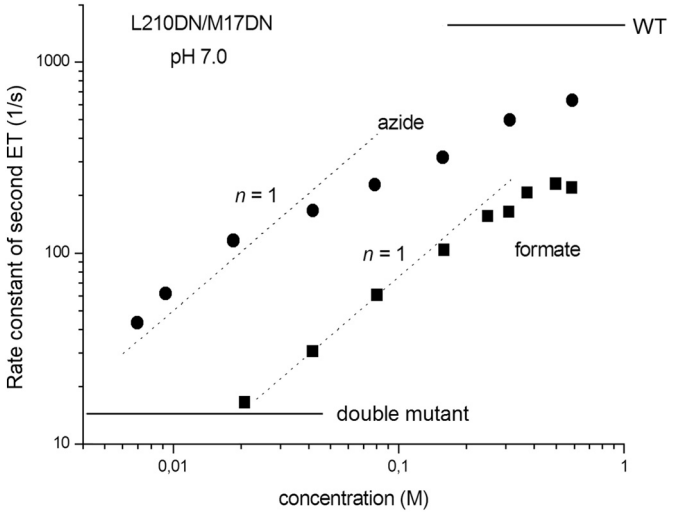

Fig. 4. Rescue of the proton transfer by small acids azide and formate in RC of severely blocked transfer pathway beneath the protein surface by double mutant L210DN/M17DN. The proton transfer is the rate limiting step of the measured second electron transfer (ET) indicated by a horizontal line. The WT level is also shown. Symbols: ● (azide) and ■ (formate). Conditions: 1.2 μM RC, 40 μM UQ_{10}, 0.02% TX, 20 mM KCl and 10 μM ethyl ferrocene or 100–400 μM ferrocene depending on the rate of the 2nd ET.

the intercept of the straight line show significant changes (Fig. 5 left). Systematic decrease of the derived energetic parameters of the free energy change $\Delta G_o^{\#}$, enthalpy change $\Delta H_o^{\#}$ and entropy change $T{\cdot}\Delta S_o^{\#}$ of activation can be derived in another proton transfer mutant L210DN/M17DN as a function of azide concentration (Fig. 5 right). The 100 mM azide decreases the entropy of activation by $T{\cdot}\Delta S_o^{\#} = -3.36$ kcal/mol indicating the ordering of the structure in the activated complex. The observed decrease of the enthalpy and the entropy has opposite tendency on the free energy gap ($\Delta G_o^{\#} = \Delta H_o^{\#} - T{\cdot}\Delta S_o^{\#}$): while the change of the enthalpy decreases, that of the entropy increases the free energy of activation. The enthalpy change $\Delta H_o^{\#}$ has larger effect on the change of the free energy of activation $\Delta G_o^{\#}$ than that of the entropy term $T{\cdot}\Delta S_o^{\#}$.

4. Discussion

4.1. Bound rescuing agent as part of the acidic cluster

The Q_B quinone binding site is deeply buried in the RC and is separated from the aqueous phase by a web of > 20 acidic residues whose ionization states are strongly connected electrostatically [18,35–38]. The protonation is usually coupled to conformational equilibrium that is part of a general mechanism for efficient pH sensing and regulation in proteins [39]. The high internal buffering capacity and connectivity make the system resistant to mutational changes designed to modify the charge environment of Q_B [40] and robust for proton transfer pathways [5,17]. The protons are collected from the solution and "funneled" them to different entry points of possible proton-transfer pathways [10,41] by an "H^+-collecting antenna" [42,43]. The protonatable residues that are up to 1–1.5 nm apart from each other can form proton-attractive domains and share the proton at a very fast rate, exceeding the upper limit of diffusion controlled reactions [44,45]. Water molecules have been shown to be part of these transfer pathways [11].

An intriguing aspect could be the comparison of the proton uptake by the bacterial RC with that at the acceptor side of photosystem II (PSII). As the photosystem II lacks an H subunit homolog, access to the surface is provided through a single residue, His-252 of the D1 subunit (homologous with L, [46]). Moreover, since the plant membranes are tightly appressed, the solvent accessibility is more restricted than in the bacterial system. In addition, the residue in the key position homologous to L212Glu in the bacterial RC is alanine and thus unable to protonate. Therefore, water molecules must be proposed to play a more important mechanistic role in proton delivery to Q_BH^- in PSII [47] than in bacterial RC.

The collective behavior of multiple acidic residues results in strongly anticooperative proton binding and unspecific disappearance of the high pH band of proton uptake observed in several mutants [17]. In the presence of small acids (azide or formate), unusual titration curve of L212GluH/(…) was observed (Fig. 2). Similar non-monotonic titration of small molecules like diethylenetriamine pentaacetate (DTPA) was described earlier [48,49]. The puzzling back titration of L212Glu in the presence of azide or formate can be considered as the collective response of the acidic cluster to the chemical rescue. We propose that the back titration of protons arises from the natural consequence of adding a new member to the interactive proton cluster. To establish a

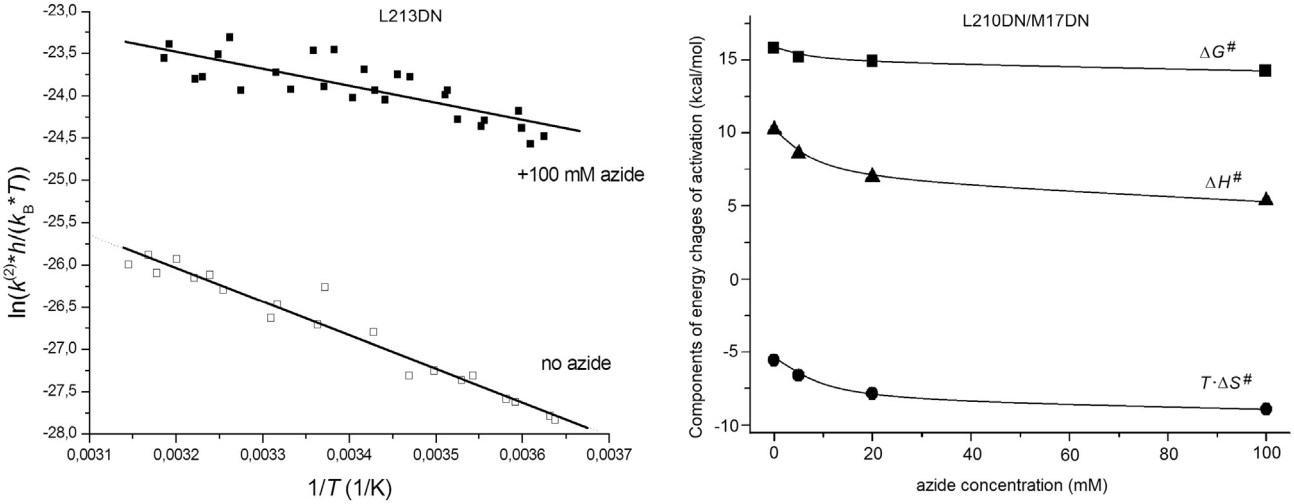

Fig. 5. Temperature-dependence (Eyring plot) of the rate constant of the 2nd electron transfer $k^{(2)}$ in L213DN mutant without (□) and with (■, 100 mM) rescue of the proton transfer by small acid azide (left panel) and free energy ($\Delta G^{\#}$), enthalpy ($\Delta H^{\#}$) and entropy ($T{\cdot}\Delta S^{\#}$) of activation of $k^{(2)}$ in L210DN/M17DN double mutant as function of the concentration of the rescuing agent azide (right panel). The energy changes of the activation of L213DN in untreated and by 100 mM azide treated cases are $\Delta G^{\#} = 15.7$ kcal/mol, $\Delta H^{\#} = 7.92$ kcal/mol and $T{\cdot}\Delta S^{\#} = -7.74$ kcal/mol and $\Delta G^{\#} = 13.7$ kcal/mol, $\Delta H^{\#} = 3.11$ kcal/mol and $T{\cdot}\Delta S^{\#} = -10.6$ kcal/mol, respectively.

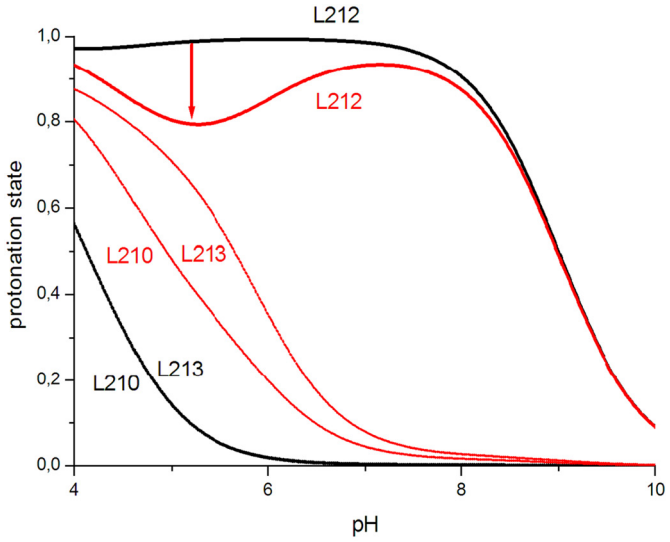

residues	L212	L213	L210	small acid
L212	pH – 5.0	-1.1	-0.9	0
L213	-1.1	pH – 4.0	-0.1	-0.4
L210	-0.9	-0.1	pH – 4.0	-0.7
small acid	0	-0.4	-0.7	pH – 3.0

Fig. 6. Model calculation (see Eq. (4)) of the pH dependence of the protonation states of the residues of the cluster consisting of three protonatable groups (L212, L213 and L210) in the absence (black lines) and presence (red lines) of a small acid bound to the cluster (top panel). The intrinsic pK_a values of the acidic residues and the interaction energies (in units of 60 meV) are given in the table (bottom panel, 60 meV correspond to 1 pH unit). The arrow shows the extent and pH region of the back titration of protons on L212 in the interacting system upon connection of an additional (rescuing) acidic residue of pK_a = 3.0 to the cluster.

quantitative point, a simplified model will be used to show that the complex interaction in the cluster accounts for the observed phenomenon.

In the model calculation, three interacting groups ("core Q_B cluster") including L212Glu are considered that is extended by a small rescuing acid bound to the RC (Fig. 6). The interaction matrix **M**(pH) includes the intrinsic pK_a values of the residues and the mutual interaction energies. The unprotonated acid groups mutually shift their pK_a's toward higher values. L212Glu describes a complex protonation behavior with an apparent pK highly (by about 3 pH units) shifted from the intrinsic value that is in good agreement with the pH profile of the rate constant of the charge recombination (Fig. 2). The cumulated interactions of smaller (about 1 pH unit) interaction energies within the cluster result in the observed large pK shift.

As the rescuing small acid is bound to one of the amino acids at or close to the protein surface [21], it will become part of the strongly interacting acidic cluster. By taking reasonable distance-dependent interaction energies with other members of the cluster, a modified pattern of the protonation state of L212Glu can be derived with strong indication of the back-titration. The reversed titration of protons at L212Glu is a unique consequence of binding of the small acids to the RC and is manifested as local decrease of the back reaction rate (Fig. 2). Some small acids (e.g. azide) can shift additionally the operational pK of the residues in the cluster. The simple model calculation demonstrates that involvement of agents that rescue the interacting proton acceptor cluster may modify the connectivity and account for the complex pH-dependence of the charge recombination controlled primarily by the protonation state of L212Glu.

4.2. Size and charge limitations of the rescuing agents

Due to the small internal volume of the proton channel, only small agents can be used for rescue. The deeper the lesion in the proton pathway, the smaller is the chance for the rescuer to penetrate to this point and to recover the proton transfer activity. It was demonstrated that the activity of impaired RC could be fully or partially reactivated by small weak acids or buffers, such as azide or tricine. In addition to the small size, the ionic character of the rescuer also plays an important role.

The damage in form of simultaneous mutations of H126His and H128His to Ala at the putative H^+ entry site on the protein surface caused 4 to 10 times deceleration of the second electron transfer [20]. The mutation neutralized the two surface histidine residues and a variety of cationic buffers (e.g. imidazole) were able to restore the electron transfer rates to near wild-type levels. As a matter of fact, the inhibitory effects were initially not seen when the catalytic activity was assayed in the standard (15 mM) Tris-HCl buffer, because the amino group of Tris in equilibrium between $NH_2 \leftrightarrow NH_3^+$ states acted as a proton donor and rescued the effects of the His changes on the proton uptake. As the mutations occurred at the surface of the protein, the cationic Tris buffer of relatively small concentration could rescue the proton transfer to Q_B. However, if the proton gate is blocked by divalent cation Cd^{2+}, the cationic buffer (Tris) can be used with much less efficiency and the zwitterionic tricine remains a good rescuer (Fig. 3). Interrupting the proton transfer chain deeper below the surface (at L213), the Tris buffer exhibited no rescuing capacity and even tricine accomplishes only highly restricted recovery.

The advantage of the zwitterionic nature of the rescuing acids can be well demonstrated by azide that has proved to be one of the most effective agents. Out of the 3 nitrogen atoms of azide, the inner nitrogen atom is positively charged and can form ionic interaction with other electronegative (e.g. oxygen) atoms. The 2 negatively charged outer nitrogen atoms can participate in hydrogen bonding interactions:

$$^{H}\cdots\mathbf{N} = \mathbf{N}^{+} = \mathbf{N}^{-}\cdots^{H}.$$

Based on the pH-dependence of the rate constant of the charge recombination (Fig. 2), the azide showed two distinct effects: the bound anion N_3^- had an electrostatic influence on the protonatable residues causing a moderated upward pK shift and the acid form N_3H modified the protonation pattern of L212Glu resulting in back titration. The question arises what function of N_3^-/N_3H is crucial for rescue of the activity of the RC. The formate $HCOO^-$ showed no sign of electrostatic effect on the protonatable groups in the cluster, but formic acid HCOOH (the simplest carboxylic acid) demonstrated similar effectiveness in the recovery of the proton delivery as the acid form of azide. This observation indicates that the proton delivery function of the added acid species and not the electrostatic perturbation determines the reactivation of the impaired RC.

This can be rationalized by the relative binding properties of the rescuing weak acid (AH) and its deprotonated form (A^-) to the RC. AH and A^- both bind very weakly (dissociation constant ~1 M) and in competition for the same binding site [21]. For acids of pK_a ~ 4 in the investigated pH range (> 7), the concentration of the protonated species is small, the anion is the overwhelming species present and the total salt concentration is very high. The relative binding affinities of the neutral acids and anionic bases may differ in azide and formate. In azide, the binding constants for AH and A^- might be commeasurable even for the weak binding affinities involved. Therefore, the RCs become occupied by both AH and A^- in well balanced manner leading to contributions to proton delivery and electrostatic control of the

transfer, respectively. In the case of the formic acid, the binding affinity of A^- could be substantially weaker than that of AH and the RC will be dominantly occupied by AH resulting in strong contribution to proton delivery function and negligible electrostatic effect in the acidic cluster.

4.3. Entropy decrease associated with rescue

Our findings show that small acids and salts in large concentrations enhance the rate of H^+ transfer from the aqueous phase to the deeply buried Q_B^- semiquinone in proton transfer mutants of RC. From thermodynamic point of view, it is attributed to the decrease of the free energy of activation ($\Delta G_o^{\#} = \Delta H_o^{\#} - T{\cdot}\Delta S_o^{\#}$), whose enthalpic ($\Delta H_o^{\#}$) and entropic ($T{\cdot}\Delta S_o^{\#}$) components demonstrate opposite tendencies (Fig. 5). $\Delta H_o^{\#}$ decreases significantly due to binding of the rescuing protonated agents to critical points of the fragmented and loosely connected H-bond network making the pathway energetically more compact and suited for transfer of H^+ ions. The decrease amounts of 60% in L213DN (100 mM azide) and 50% in L210DN/M17DN double mutant (100 mM azide). Similarly, decrease of the entropy of activation $\Delta S_o^{\#} < 0$ was measured indicating a more ordered and rigid structure in the activated complex. A not insignificant part of the decrease (~30%) is attributed to the decrease of the number of configurations of alternative proton transfer pathways that are not fast enough for transferring protons. The change in the entropy of activation ($T{\cdot}\Delta S_o^{\#} < 0$) will enhance the free energy of activation. As the decrease of the enthalpy of activation is larger than that of the entropy of activation, the free energy of activation will decrease and manifest the proton rescue effect of small acids and salts in proton transfer mutants.

From the measured entropy changes of the activated complex in the absence and in the presence of azide, we can give a rough estimate to the reduction of proton transfer pathways upon chemical rescue. The change of entropy is connected to the thermodynamic probability (w) of the microstates (number of pathways) in a macrostate: $\Delta S_o^{\#} = k_B{\cdot}\ln w$, where k_B is the Boltzmann's constant. The entropy changes of activation due to 100 mM azide are –11.2 cal/mol/K in L210DN/M17DN double mutant and −9.6 cal/mol/K in L213DN mutant (Fig. 5). These values correspond to reduction of the number of proton pathways by a factor of ($1/w$ =) 270 (L210DN/M17DN) and 122 (L213DN). The rescue effect of azide in 100 mM concentration is twofold: it decreases the enthalpy of activation by delivering protons to the defected sites and selects some proton pathways (~0.5–1%) out of the numerous alternate routes making these pathways available for proton delivery only.

5. Conclusions

The results of chemical rescue tell us that we must take into consideration the combined spatial-energetic arrangement of acidic residues in the proton delivery system. If the components are properly arranged in both space (bucket brigade) and energy (pK difference), the protons will be transported with high rates that assures very efficient proton uptake of the transient semiquinone buried in the Q_B pocket. Although the principle of operation of the proton delivery system resembles that of the migration of electronic excitation energy in the light harvesting system [50], the flexibility is much smaller: in wild type RCs, there is practically a single proton pathway with no alternate routes. In the case of surface defects of the proton delivery pathway, the small neutral or zwitterionic acids/buffers do not open alternate pathways but reactivate the injured pathway. In proton transfer mutants, however, the rescue is partial and focused on a small fraction (1%) of the alternate routes.

Transparency document

The Transparency document associated with this article can be found, in online version.

Acknowledgements

I'm grateful to Profs. James Smart (Department of Biological Sciences, University of Tennessee at Martin, USA), Colin Wraight (†2014) and Gábor Sipka (Biological Research Center Szeged, Hungary) for reading the text, mutants and Fig. 1, respectively and gratefully acknowledge support from COST (CM1306) and EFOP-3.6.2-16-2017-0005.

References

[1] C.T. Supuran, Structure and function of carbonic anhydrases, Biochem. J. 473 (2016) 2023–2032.
[2] O.A. Sineshchekov, E.G. Govorunova, H. Li, J.L. Spudich, Bacteriorhodopsin-like channelrhodopsins: alternative mechanism for control of cation conductance, Proc. Natl. Acad. Sci. U. S. A. 114 (45) (2017) 9512–9519.
[3] M. Wikström, C. Ribacka, M. Molin, L. Laakkonen, M. Verkhovsky, A. Puustinen, Gating of proton and water transfer in the respiratory enzyme cytochrome c oxidase, Proc. Natl. Acad. Sci. U. S. A. 102 (2005) 10478–10481.
[4] M.R.A. Blomberg, P.E.M. Siegbahn, Proton pumping in cytochrome *c* oxidase: energetic requirements and the role of two proton channels, Biochim. Biophys. Acta Bioenerg. 1837 (7) (2016) 1165–1177.
[5] P. Maróti, Govindjee, The two last overviews by Colin Allen Wraight (1945–2014) on energy conversion in photosynthetic bacteria, Photosynth. Res. 127 (2) (2016) 257–271.
[6] C.A. Wraight, Chance and design—proton transfer in water, channels and bioenergetic proteins, Biochim. Biophys. Acta 1757 (2006) 886–912.
[7] P. Maróti, D.K. Hanson, L. Baciou, M. Schiffer, P. Sebban, Proton conduction within the reaction centers of *Rhodobacter capsulatus*: the electrostatic role of the protein, Proc. Natl. Acad. Sci. U. S. A. 91 (12) (1994) 5617–5621.
[8] M.L. Paddock, G. Feher, M.Y. Okamura, Proton transfer pathways and mechanism in bacterial reaction centers, FEBS Lett. 555 (2003) 45–50.
[9] C.A. Wraight, M. Wikström (Ed.), Intraprotein Proton Transfer – Concepts and Realities From the Bacterial Photosynthetic Reaction Center, "Biophysical and Structural Aspects of Bioenergetics", RSC Biomolecular Science Series, Royal Society of Chemistry, Cambridge, England, 2005.
[10] Q. Xu, H.J. Axelrod, E.C. Abresch, M.L. Paddock, M.Y. Okamura, G. Feher, X-ray structure determination of three mutants of the bacterial photosynthetic reaction centers from *Rb. sphaeroides*: altered proton transfer pathways, Structure 12 (2004) 703–715.
[11] E. Nabedryk, J. Breton, Coupling of electron transfer to proton uptake at the Q_B site of the bacterial reaction center: a perspective from FTIR difference spectroscopy, Biochim. Biophys. Acta 1777 (10) (2008) 1229–1248.
[12] H. Ishikita, E.W. Knapp, Variation of Ser-L223 hydrogen bonding with the Q_B redox state in reaction centers from *Rhodobacter sphaeroides*, J. Am. Chem. Soc. 126 (2004) 8059–8064.
[13] Z. Zhu, M.R. Gunner, Energetics of quinone-dependent electron and proton transfers in *Rhodobacter sphaeroides* photosynthetic reaction centers, Biochemistry 44 (2005) 82–96.
[14] M.L. Paddock, M. Flores, R. Isaacson, C. Chang, E.C. Abresch, M.Y. Okamura, ENDOR spectroscopy reveals a light induced movement of the H-bond from Ser-L223 upon forming the semiquinone (Q_B) in reaction centers from *Rhodobacter sphaeroides*, Biochemistry 46 (2007) 8234–8243.
[15] E. Martin, A. Baldansuren, T.J. Lin, R.I. Samoilova, C.A. Wraight, S.A. Dikanov, P.J. O'Malley, Hydrogen bonding between the Q_B site ubisemiquinone and Ser-L223 in the bacterial reaction center: a combined spectroscopic and computational perspective, Biochemistry 51 (2012) 9086–9093.
[16] M.Y. Okamura, M.L. Paddock, M.S. Graige, G. Feher, Proton and electron transfer in bacterial reaction centers, Biochim. Biophys. Acta 1458 (2000) 148–163.
[17] H. Cheap, J. Tandori, V. Derrien, M. Benoit, P. de Oliveira, J. Köpke, J. Lavergne, P. Maróti, P. Sebban, Evidence for delocalized anticooperative flash induced proton binding as revealed by mutants at the M266His iron ligand in bacterial reaction centers, Biochemistry 46 (15) (2007) 4510–4521.
[18] P. Sebban, P. Maróti, M. Schiffer, D.K. Hanson, Electrostatic dominoes: long distance propagation of mutational effects in photosynthetic reaction centers of *Rhodobacter capsulatus*, Biochemistry 34 (1995) 8390–8397.
[19] P. Maróti, D.K. Hanson, M. Schiffer, P. Sebban, Long-range electrostatic interaction in the bacterial photosynthetic reaction Centre, Nat. Struct. Biol. 2 (1995) 1057–1059.
[20] M.L. Paddock, P. Ädelroth, G. Feher, M.Y. Okamura, J.T. Beatty, Determination of proton transfer rates by chemical rescue: application to bacterial reaction centers, Biochemistry 41 (2002) 14716–14725.
[21] E. Takahashi, C.A. Wraight, Small weak acids reactivate proton transfer in reaction centers from *Rhodobacter sphaeroides* mutated at Asp^{L210} and Asp^{M17}, J. Biol. Chem. 281 (7) (2006) 4413–4422.
[22] Á. Maróti, C.A. Wraight, P. Maróti, The rate of second electron transfer to Q_B^- in bacterial reaction center of impaired proton delivery shows hydrogen-isotope effect, Biochim. Biophys. Acta 1847 (2015) 223–230.
[23] Á. Maróti, C.A. Wraight, P. Maróti, Protonated rhodosemiquinone at the Q_B binding site of the M265IT mutant reaction center of photosynthetic bacterium *Rhodobacter sphaeroides*, Biochemistry 54 (12) (2015) 2095–2103.
[24] C.M. Maupin, N. Castillo, S. Taraphder, C. Tu, R. McKenna, D.N. Silverman,

G.A. Voth, Chemical rescue of enzymes: proton transfer in mutants of human carbonic anhydrase II, J. Am. Chem. Soc. 133 (16) (2011) 6223–6234.
[25] Sh. Ferguson-Miller, C. Hiser, J. Liu, Gating and regulation of the cytochrome *c* oxidase proton pump, Biochim. Biophys. Acta 1817 (2012) 489–494.
[26] J. Geng, A. Liu, Heme-dependent dioxygenases in tryptophan oxidation, Arch. Biochem. Biophys. 544 (2014) 18–26.
[27] S. Kim, J. Liang, B.A. Barry, Chemical complementation identifies a proton acceptor for redox-active tyrosine D in photosystem II, Proc. Natl. Acad. Sci. U. S. A. 94 (1997) 14406–14411.
[28] A. Peracchi, How (and why) to revive a dead enzyme: the power of chemical rescue, Curr. Chem. Biol. 2 (2008) 32–49.
[29] M.L. Paddock, M.S. Graige, G. Feher, M.Y. Okamura, Identification of the proton pathway in bacterial reaction centers: inhibition of proton transfer by binding of Zn^{2+} or Cd^{2+}, Proc. Natl. Acad. Sci. U. S. A. 96 (1999) 6183–6188.
[30] L. Gerencsér, P. Maróti, Retardation of proton transfer caused by binding of the transitionmetal ion to the bacterial reaction center is due to pK_a shifts of key protonatable residues, Biochemistry 40 (2001) 1850–1860.
[31] E. Takahashi, C.A. Wraight, A crucial role for AspL213 in the proton transfer pathway to the secondary quinone of reaction centers from *Rhodobacter sphaeroides*, Biochim. Biophys. Acta 1020 (1990) 107–111.
[32] P. Maróti, C.A. Wraight, Flash-induced H^+ binding by bacterial photosynthetic reaction centers: comparison of spectrophotometric and conductimetric measurements, Biochim. Biophys. Acta 934 (1988) 314–328.
[33] L. Gerencsér, B. Boros, V. Derrien, D.K. Hanson, C.A. Wraight, P. Sebban, P. Maróti, Stigmatellin probes the electrostatic potential in the Q_B site of the photosynthetic reaction center, Biophys. J. 108 (2015) 379–394.
[34] A. Taly, P. Sebban, J.C. Smith, G.M. Ullmann, The position of Q_B in the photosynthetic reaction center depends on pH: a theoretical analysis of the proton uptake upon Q_B reduction, Biophys. J. 84 (2003) 2090–2098.
[35] P. Beroza, D.R. Fredkin, M.Y. Okamura, G. Feher, Electrostatic calculations of amino acid titration and electron transfer, $Q_A^- Q_B \rightarrow Q_A Q_B^-$ in the reaction center, Biophys. J. 68 (1995) 2233–2250.
[36] E.G. Alexov, M.R. Gunner, Calculated protein and proton motions coupled to electron transfer: electron transfer from Q_A^- to Q_B in bacterial photosynthetic reaction centers, Biochemistry 38 (1999) 8253–8270.
[37] H. Ishikita, G. Morra, E.W. Knapp, Redox potential of quinones in photosynthetic reaction centers from *Rhodobacter sphaeroides*: dependence on protonation of Glu-L212 and Asp-L213, Biochemistry 42 (2003) 3882–3892.
[38] C.A. Wraight, M.R. Gunner, The acceptor quinones of purple photosynthetic bacteria: structure and spectroscopy, in: C.N. Hunter, F. Daldal, M.C. Thurnauer, J.T. Beatty (Eds.), Advances in Photosynthesis and Respiration: The Purple Phototrophic Bacteria, Springer, Dordrecht, The Netherlands, 2009, pp. 379–405.
[39] J. Liu, J. Swails, J.Z.H. Zhang, X. He, E. Adrian, A.R. Roitberg, A coupled ionization-conformational equilibrium is required to understand the properties of ionizable residues in the hydrophobic interior of staphylococcal nuclease, J. Am. Chem. Soc. 140 (5) (2018) 1639–1648.
[40] E. Alexov, J. Miksovska, L. Baciou, M. Schiffer, D.K. Hanson, P. Sebban, M.R. Gunner, Modeling the effects of mutations on the free energy of the first electron transfer from Q_A to Q_B^- in photosynthetic reaction centers, Biochemistry 39 (2000) 5940–5952.
[41] E.M. Krammer, M.S. Till, P. Sebban, G.M. Ullmann, Proton-transfer pathways in photosynthetic reaction centers analyzed by profile hidden Markov models and network calculations, J. Mol. Biol. 388 (3) (2009) 631–643.
[42] P. Ädelroth, P. Brzezinski, Surface-mediated proton-transfer reactions in membrane-bound proteins, Biochim. Biophys. Acta 1655 (2004) 102–115.
[43] M. Brändén, T. Sandén, P. Brzezinski, J. Widengren, Localized proton microcircuits at the biological membrane-water interface, Proc. Natl. Acad. Sci. U. S. A. 103 (2006) 19766–19770.
[44] P. Maróti, C.A. Wraight, Kinetics of H^+ ion binding by the $P^+Q_A^-$ state of bacterial photosynthetic reaction centers: rate limitation within the protein, Biophys. J. 73 (1997) 367–381.
[45] M. Gutman, E. Nachliel, R. Friedman, The dynamics of proton transfer between adjacent sites, Photochem. Photobiol. Sci. 5 (2006) 531–537.
[46] Y. Umena, K. Kawakami, J.R. Shen, N. Kamiya, Crystal structure of oxygen-evolving photosystem II at a resolution of 1.9 Å, Nature 473 (2011) 55–60.
[47] K. Linke, F.M. Ho, Water in photosystem II: structural, functional and mechanistic considerations, Biochim. Biophys. Acta Bioenerg. 1837 (1) (2014) 14–32.
[48] A. Onufriev, D.A. Case, G.M. Ullmann, A novel view of pH titration in biomolecules, Biochemistry 40 (12) (2001) 3413–3419.
[49] G.M. Ullmann, E. Bombarda, pK_a a values and redox potentials of proteins. What do they mean? Biol. Chem. 394 (5) (2013) 611–619.
[50] T. Brixner, J. Stenger, H.M. Vaswani, M. Cho, R.E. Blankenship, G.R. Fleming, Two-dimensional spectroscopy of electronic couplings in photosynthesis, Nature 434 (7033) (2005) 625–628.